

Assessment of AC Losses in Cobalt Ferrite Nanoparticles Using a Varying Frequency Induction Heater

*Heba Kahil¹, H.M. El_Sayed¹

¹Departement of physics, Faculty of Science, Ain Shams University, 11566, Abassia, Cairo, Egypt

Abstract: During the last years, there has been a growing interest in studying the heat dissipation of magnetic nanoparticles on exposure to electromagnetic fields. This is of particular importance for their subsequent use in the constitution of ferrofluids for magnetic fluid hyperthermia (MFH). This study presents the synthesis and characterization of a cobalt ferrite sample with a nanoparticle diameter of 13.65 nm. The AC loss ability of the sample in the frequency range 100 to 250 kHz has been assessed. For this purpose a customized self-oscillating induction heater has been constructed. The details of the construction and calibration of the alternating magnetic field are described in this work. The maximum field intensity H achieved by this assembly is 3.5 (kA/m) in the frequency range 100 to 250 kHz. This miniature working coil was used for heating magnetic nano-powders via relaxational losses. The rise in temperature with time of the sample over the specified frequency range is depicted. The sample showed a temperature rise of 82°C and a field of 244.6 kHz at a field intensity of 3.5kA/m. Therefore, the designed induction heater proved to meet the requirements for future use in MFH.

Keywords: AC losses, Brownian loss, Cobalt ferrite, Induction heater, magnetic nanoparticles, Neel loss

I. Introduction

Cobalt ferrite is one of the promising candidates for magnetic fluid hyperthermia [1-2]. Its preparation via a variety of routes has been the interest of several authors [3]. Co-precipitation method is utilized here [4-5] as it has the capability of producing fine particles [6] in a narrow size distribution suitable for the purpose of heating via relaxational losses [7]. Cobalt ferrite has an inverse spinel structure [8] that is known for its remarkable properties including high chemical stability [9], biocompatibility [10] and tunable magnetic properties [11].

Induction heating refers to the heating of an object inserted in a working coil through which time varying current is passed. Several applications in research and industry are based on this phenomenon [12]. Few applications include induction welding, cooking, sealing, brazing and heating of metals in induction furnaces [13-14]. Thermal energy dissipated in metallic samples on exposure to an alternating electromagnetic field (AEMF) is attributed to one or more of several mechanisms including Eddy currents, hysteresis, and relaxational losses. These mechanisms utilize the alternating magnetic component of the applied AEMF and the prevailing loss mechanism is determined by the sample properties.

The current study presents the design and construction of a moderate power induction heater with a miniature working coil. The synthesized cobalt ferrite sample is utilized in this study to prove the applicability of the device and test the feasibility of the future use of the sample for magnetic fluid hyperthermia.

The induction heater is a modified form of the Royer type resonant oscillator invented and patented by George Royer in 1954 [15]. The aim of the invented circuit at that time was to convert direct current (DC) to alternating current (AC). The circuit was very simple as it utilized two transistors, a center tapped transformer with identical windings, feedback windings a saturable core and a secondary winding [16]. This self-oscillating [17-18] push-pull converter gave a square pulse on the secondary windings of the transformer. A push-pull converter refers in general to any converter with bidirectional excitation of the transformer. The frequency f of the output square signal depends on the DC input voltage (V_{in}) that is applied across the center tap with similar windings, each with a number of turns (N) and B_w is the operating magnetic induction intensity (T), S_N is the magnetic core effective cross-sectional area. The frequency f of the output is calculated from the following relation [9]

$$f = \frac{V_{in}}{4NB_w S_N} \quad 1$$

This square output voltage in the Royer oscillator is not required; instead, a high sinusoidal AC current flowing in the working coil at a specified frequency is desired to heat the material via one or more of the previously mentioned mechanisms. Therefore, the circuit is modified to meet our needs as shown in section 2.2. Heat dissipation in metals and metal oxides on exposure to AEMF is generally attributed to one or more of the following mechanisms:

- 1) Eddy currents loss, the electrically conductive material responds according to Faraday's and Lenz's laws and the dissipated power is given by [20]:

$$P_{ED} = \frac{(\mu\pi dfH_0)^2}{20\rho} \quad 2$$

where μ , d and ρ are the permeability, diameter and resistivity of the material respectively.

- 2) Hysteresis loss is given by equation (3) [21] where M is the magnetization of the sample and μ_0 is the permeability of free space.

$$P = \mu_0 \oint MdH \quad 3$$

- 3) Relaxational losses constitute two mechanisms namely Brownian rotation and Neel relaxation. Brownian rotation refers to the rotational of the particle as whole against a viscosity barrier in the alternating magnetic field AMF with a relaxation time given by [22]:

$$\tau_B = \frac{3\eta V_H}{kT} \quad 4$$

Where η is the viscosity of the dispersing material (solvent) and k is the Boltzmann constant, T is the absolute temperature and V_H is the hydrodynamic volume of the particle. Neel relaxation is the rotation of the magnetic moments towards and away from the direction of magnetization with a relaxation time given by [23], where V_M is the volume of the magnetic core.

$$\tau_N = \tau_0 e^{\frac{kV_M}{kT}} \quad 5$$

Relaxational losses are the heating mechanisms responsible for heat dissipation in the obtained sample with an equivalent relaxation time given by [24]. According to equation (11), the shorter time dominates.

$$\tau = \frac{\tau_B \tau_N}{\tau_B + \tau_N} \quad 6$$

The power loss due to relaxational mechanisms is given by [25]

$$P = \mu_0 \pi \chi'' f H_0^2 \quad 7$$

where H_0 is the applied field intensity at the frequency f and χ'' is the imaginary part of the complex susceptibility

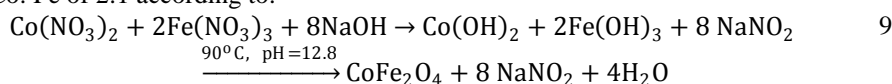
$$\chi'' = \frac{\omega\tau}{1 + (\omega\tau)^2} \chi_0 \quad 8$$

where χ_0 is the DC susceptibility. Equations (7, 8) depict the dependence of the dissipated power on the total or the equivalent relaxation time τ .

II. Experimental Work

2.1 Experimental procedure

Cobalt ferrite is prepared by the co-precipitation [4, 5, 9] method from iron and cobalt nitrate precursors with a ratio of Co: Fe of 2:1 according to:



The salts are dissolved separately in distilled water then added together. NaOH (precipitating agent) is added drop by drop under continuous stirring until pH value reaches 12.8. Heating starts and the solution is held at 90°C for two hours till the formation of a black precipitate representing the desired magnetic phase. The sample is subsequently washed several times with distilled water and dried.

2.2 Circuit design and operation

A Mazzilli inverter was first proposed by Vladimiro Mazzilli [26] is a combination between Royer oscillator and induction – capacitor metal oxide semiconductor L-C MOS oscillator [27]. It allows large currents to oscillate back and forth between the capacitor and the working coil producing a large alternating magnetic field in the working coil by which the sample is heated. Fig.1. shows the used induction heater which is practically a Mazzilli inverter with the secondary coil removed.

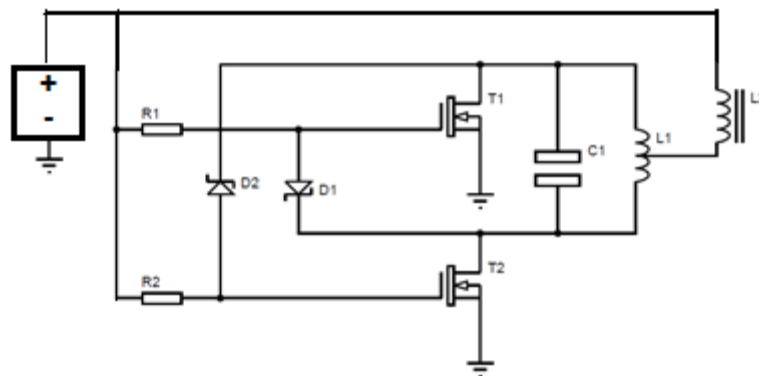


Fig. 1: the used induction heater as a modified Mazzili inverter

The working coil is a center-tapped transformer. Though working with center-taped transformers is not as simple as regular transformers, it is necessary for the operation of the circuit. DC voltage from a rectified source is applied to the center-tap of the working coil thus; current flows through both of its sides and equal DC voltage appears simultaneously on the gates of both metal oxide semiconductor (MOSFETs) (T_1 & T_2) along with the voltage supplied from the source via R1 and R2 to switch the MOSFETs on. As the two MOSFETs are not identical they have different response times causing one of them to switch before the other. The MOSFET that is in the ON state (say T_1) will deprive the other (T_2) from the current leading the later to be in an OFF state.

Each side of the capacitor is connected to the gate of the MOSFET on the opposite side; the MOSFETs are fed with signals that are 180° out of phase at any instant. The orientation of the diode (D1) allows the negative half cycle of the signal to reach the N-type gate to retain it in the ON state for this half cycle, whereas T_2 is retained in the OFF state. In the next half cycle no signal is fed to T_1 whereas, T_2 is fed with the negative half of the signal which allows T_2 to be switched ON for that half cycle. The process is repeated in the onset of the next cycle by switching T_1 to the ON state. The operation frequency f (the frequency of the large current in the working coil) is the resonant frequency of the tank circuit and is given by:

$$f = \frac{1}{2\pi\sqrt{LC}} \quad 10$$

where L is the inductance of the coil and C is the capacitance of the capacitor. It is apparent from the operation of the circuit that this oscillator is a zero voltage switch (ZVS), this means that switching of the MOSFETs occurs with almost zero voltage across them. This soft switching in contrast to hard switching, leads to remarkably less switching losses. This property is very important especially at high frequencies as the power loss increases with frequency [11]. The circuit is a self-oscillating converter [17, 18], thanks to the presence of the capacitor C that constitutes a resonant circuit with the working coil which enables the circuit to act as a ZVS oscillator. ZVS has proved to be efficient in a variety of applications [28-29] due to the enhanced efficiency and the reduction in the number of used components [30] thus making the circuit less costly and more compact. The positive feed-back ensures circuit stability as it is possible to feed-back the proper amount of voltage for constant amplitude oscillations because if the oscillations increase, the biasing of the gate increases and consequently decreases the gain leading to a decreased gate biasing in the next cycle in a robust manner.

MOSFETs perform well in ZVS circuits because they possess inherently low ON resistance ($R_{ds(on)}$); when they are in the OFF state they are open circuit and when they are ON they are almost a short circuit with a very little resistance (few milliohms) [31]. The timing of the circuit is a crucial matter for stable operation. If both transistors are ON, this definitely leads to a short circuit and if they are both OFF high voltages appear due to back EMF. Using fast transistors as is the case of (MOSFETs) does not allow enough time for the back EMF to charge the capacitor of the transformer (inherent in the windings) and the body diode of the MOSFET to high voltages. The MOSFETs T_1 and T_2 used in this study are IRFP250N purchased from International Rectifier with static drain to source resistance $R_{DS(on)} = 75\text{m}\Omega$, and maximum drain current $I_D = 30\text{ A}$ also, the voltage rating of the MOSFET is four times the power supply.

For optimized performance, other components are added to the circuit. Resistance R1 and R2 are used to limit the gate current thus protect the MOSFETs. They should not be too large as this will slow down switching of the gate. These resistors also should be high power resistors to withstand large currents through them. In this circuit 220 ohm, 0.6 watts ceramic resistors are used. The diodes D1 and D2 are responsible for discharging the gates which implies that they should have low forward drop to attain efficient discharging of the

MOSFET that is in the OFF state before the onset of the next cycle. The voltage rating of the diodes should be high as the voltage in the tank circuit rises considerably. Diodes used here are IN4007. The choke coil L2 protects the power supply unit (PSU) from the frequency oscillations [32], and also protects the gates from the sudden rise in current due to its capability of storing energy. The value of the inductance of the choke coil is chosen such that the reactance is large at the operation frequency. The coil is made by winding a thick wire around a ferrite core, some experimentation is necessary to achieve a suitable coil or the circuit may fail to oscillate.

It should be noted that the tank circuit is the part of the circuit with the highest heat dissipation. Therefore, the capacitors and the working coil should both be properly selected to withstand the rise in temperature. Concerning the capacitor, polyester capacitors are utilized as they have a high dielectric constant and dielectric strength. They also have excellent self-healing properties and good temperature stability [33]. Also parallel combinations of small capacitors to give the required capacitances help to divide the large currents and consequently decrease the heat dissipation in each capacitor. The range of the capacitances used is 300-900 nF for frequency range of 100 to 250 kHz.

It is also important to state that the circuit employs large currents and voltages; therefore caution is required to avoid electrical shocks. The MOSFETs T1 and T2 are separately mounted on heat sinks. The drain is in contact with the heat sink therefore, the two sinks should never be brought in contact. This is in addition to using thick enough wires and making them as short as possible with proper soldering.

2.3 Working coil design and experimental set up

A cross section for the setup containing the working coil, its jacket, the sample within the glass holder and the IR thermometer used in this experiment are shown in Fig. 2(dimensions shown). The coil used is a copper tube with inner diameter of 0.4 cm to allow cooling water current to flow. For a coil with number of turns n and diameter of each turn D in cm, the magnetic field H in kA/m can be calculated knowing the current I (A). In finite solenoids in general, the field intensity H is inversely proportional to the coil diameter D . The chosen diameter is the minimum diameter suitable for enclosing a test tube insulated by polystyrene jacket.

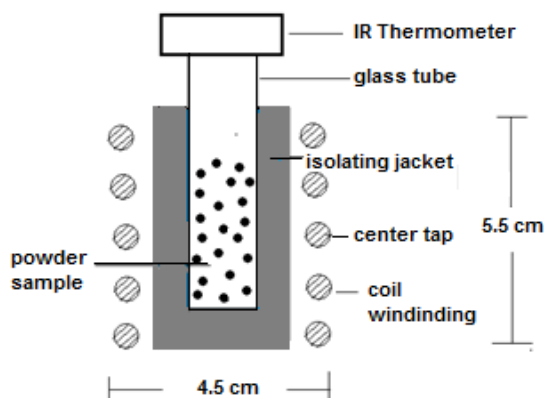


Fig. 2: cross section for experimental set up

Magnetic field calibration in the coil is performed against a DC Teslameter (Phywe Teslameter 13610-93, Germany) for low DC currents; up to 6 A. The plot of DC magnetic field strength H versus I showed a linear dependence. Current I is calculated knowing that the tank circuit operating at a certain frequency f utilizes a capacitor with capacitance C . Assuming that the capacitor discharges all its charge Q in the coil at $I = I_{\max}$ giving

$$I_{\max} = Q_{\max} \omega \tag{11}$$

or

$$I_{\max} = 2\pi f C (\sqrt{2} V_{\text{rms}}) \tag{12}$$

Where V is the AC voltage measured across the coil. Accordingly, two values of the applied current, 32 and 45 A were obtained. A linear relation was obtained between the magnetic field B in mT and the coil current I in ampere with a slope of 0.983. This implies that the field H (A/m) = 77.46 I . Therefore, the values of the two applied fields are $H_1 = 2.4$ kA/m and $H_2 = 3.5$ kA/m.

To plot a temperature profile of the cobalt ferrite nanoparticles, 2 grams of the sample in powder form are contained in a glass test tube that is inserted axially in a polystyrene foam jacket inside the working coil [34-36]. Polystyrene foam is made of expanded polystyrene beads which is a good thermal insulator material due to the abundance of trapped air molecules 98% of the volume, in addition to the fact that the large polystyrene molecules are good insulators. The coefficient of thermal conductivity k is very low ($0.033 \text{ W/(m}\cdot\text{K)}$) [37].

An infrared (IR) thermometer (FLUKE 62 Mini IR thermometer, China) is mounted over the test tube to measure the temperature ($\pm 1\%$ of the reading). IR thermometers are applicable here as they are not affected by electromagnetic radiation, the circuitry can be affected at higher fields than those utilized here. This is in contrast to thermocouples that are heated up by electromagnetic radiations giving misleading results. The IR thermometer is calibrated against an alcohol thermometer to adjust the emissivity value and the mounting position, which is also a routine check.

2.4 Characterization

The powder XRD pattern was obtained using a PHILIPS® X'Pert diffractometer, which has the Bragg-Brentano geometry and copper tube ($\lambda = 1.54 \text{ \AA}$), the operating voltage was kept at 40 kV and the current at 30 mA. The size and morphology were studied using a FEI, Tecnai, G20, transmission electron microscope (TEM) operating at 200 kV. TEM micrographs and selected area electron diffraction (SAED) pattern were obtained by dispersing nanoparticles in water for 30 min by ultrasonic agitation. The aqueous dispersion was dropped on a carbon coated copper TEM grid.

III. Results and Discussion

3.1 Sample characterization

The diffraction pattern is shown in Fig.3 (a). According to ICDD 000030864 database, the pattern shows a single phase spinel crystal structure with a lattice parameter 0.837822 nm . The crystallite size determined using Debye-Scherrer's equation [38-39] was 13 nm . TEM micrographs and electron diffraction pattern are shown in Fig. 3(b) and 3 (d) respectively. The pattern shows a high degree of crystallinity. The particle size distribution is shown in Fig.3(c) and the count is fitted with a log-normal function according to:

$$f(d) = \frac{1}{\sqrt{2\pi}\sigma d} \exp\left[-\frac{\ln^2(d/d_0)}{2\sigma^2}\right] \quad 13$$

where σ is the distribution width, d_0 median distribution and the average diameter $d_{av} = d_0 \exp(\sigma^2/2)$. The average particle size is 13.56 nm with a standard deviation of 0.14 . Since the crystallite size and the particle size are in the same order of magnitude, it can be inferred that the particles are monocrystalline.

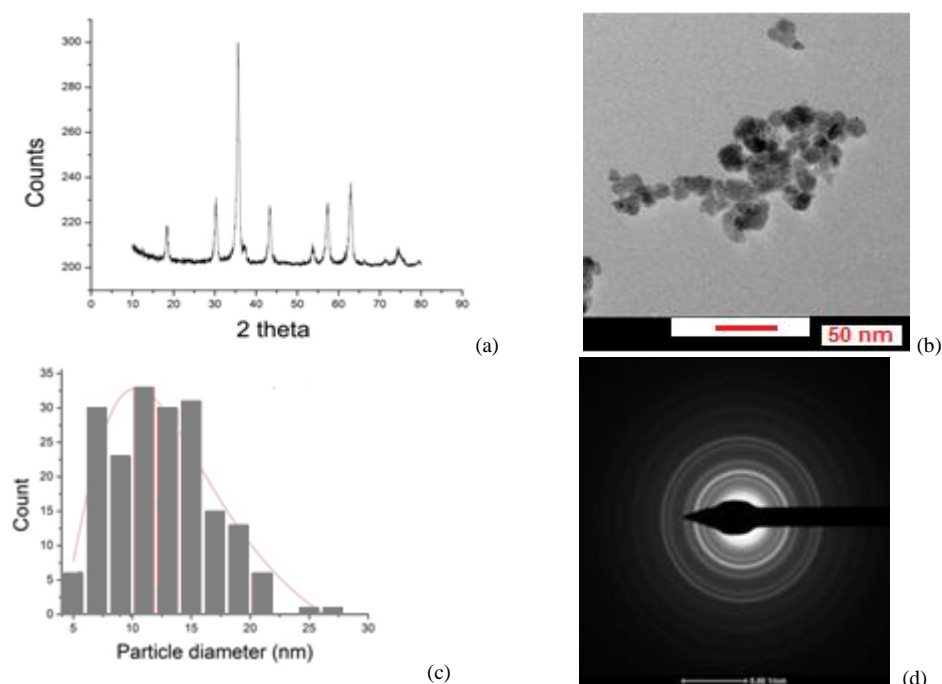


Fig. 3a) XRD pattern, b) TEM micrograph, c) size distribution of cobalt ferrite nanoparticles and lognormal fitting d) electron diffraction pattern for the cobalt ferrite sample

3.2 Assessment of AC loss

This section is concerned with proving the validity of the constructed circuit to heat small samples as well as the feasibility of the prepared sample for subsequent use in hyperthermia. The temperature rise of the cobalt ferrite sample is measured by applying the previously explained setup for an exposure time of 300 seconds. Fig. 4 shows the temperature rise with time of the cobalt ferrite sample at a field of 3.43 kA/m and frequencies 146, 163, 170, 192.2 and 244.6 kHz and the recorded rise in temperature is 52.2, 57.4, 64.2, 66, 82 K respectively. The heating ability of the sample is shown to increase with increasing frequency. Fig. 5 shows the effect of raising the field intensity H of the sample at 2.5kA/m and 3.5kA/m at a frequency of 163 kHz.

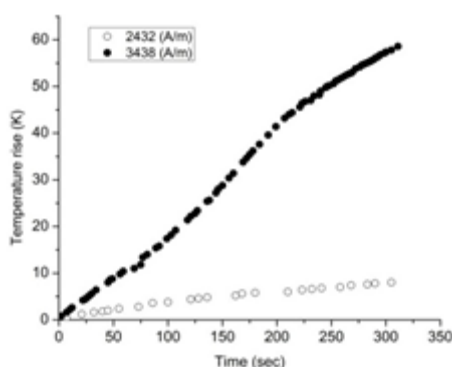


Fig. 4: rise in temperature with time for the cobalt ferrite sample at different frequencies at a field of 3.5 kA/m

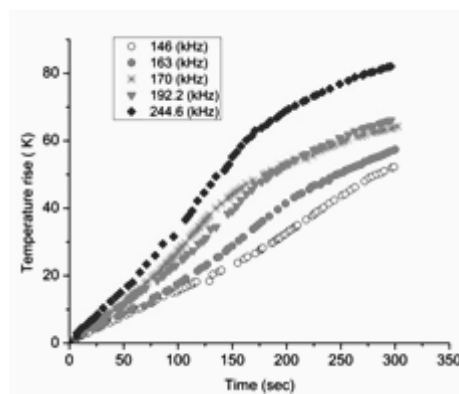


Fig. 5: effect of changing the field intensity H on the rise in temperature with time

This observed heat dissipation may be attributed to one or more of the above mentioned mechanisms. Concerning Eddy currents loss (2); since cobalt ferrite used in this study is a semiconductor with high resistivity and the diameter of the nanoparticles is small therefore, Eddy loss mechanism is excluded. The second mentioned mechanism is the hysteresis loss given by equation (3). This loss mechanism is also negligible for particles with diameters less than that of the single domain critical size (70 nm for cobalt ferrite [40]) which causes this mechanism to be excluded as well. This leaves out only relaxational losses which constitute two mechanisms namely Brownian rotation (4) and Neel relaxation (5). The prepared sample is in powder form; the samples are agglomerated which increases the hydrodynamic volume thus increasing the Brownian characteristic time (4). According to equation (6); the shorter time dominates, this in addition to the fact of lacking a viscosity barrier. For these reasons, the observed heat loss is attributed to Neel relaxation mechanism.

IV. Conclusions

A cobalt ferrite sample 13.65 nm was prepared using co-precipitation. The AC losses for the samples were successfully assessed using the constructed induction heater in the frequency range 100-250 Hz. The heater provides field intensities in the vicinity of the working coil up to 3.5 (kA/m) in this frequency range. The circuit has the advantages of being self-oscillating and only a DC power supply with an output of 30 V is required which greatly simplifies the circuit and reduces the cost. It also provided a steady output and the applied frequency could be varied in this range simply by varying the values of the capacitance. Moreover, a variety of samples as magnetic powders and small metallic parts can be heated in the working coil.

References

- [1]. S. Kuckelhaus, S. C. Reis, M. F. Carneiro, A.C. Tedesco, D.M. Oliveira, E.C.D. Lima, P.C. Morais, R.B. Azevedo, Z.G.M. Lacava, In vivo investigation of cobalt ferrite-based magnetic fluid and magnetoliposomes using morphological tests, *J.Magn. Magn.Matter.*,2004, **272-276**, p 2402-2403
- [2]. S. Amiri, H. Shokrollahi, The role of cobalt ferrite magnetic nanoparticles in medical science, *Mater. Sci. Eng.*,2013 C **33**,p1-8
- [3]. Joachim Wagner, Tina Autenrieth, Rolf Hempelmann, Core shell particles consisting of cobalt ferrite and silica as model ferrofluids [CoFe₂O₄-SiO₂ core shell particles],*J.Magn.Magn. Matter.*, 2002, **252**,p 4-6
- [4]. J. Liu, D. You, M. Yu, S. Li., Preparation and characterization of hollow glass microspheres-cobalt ferrite core-shell particles based on homogeneous coprecipitation, *Mater. Lett.*,2011, **65**,p 929-992
- [5]. G.A.El-Shobaky, A.M.Turky, N.Y.Mostafa, S.K.Mohamed, Effect of preparation conditions on physicochemical, surface and catalytic properties of cobalt ferrite prepared by coprecipitation, *J. Alloys Compd.*2011,**493**, p 415-422
- [6]. Sunil, Rohilla, Sushil Kumar, P. Aghamkar, S. Sunder, A. Agrawal, Investigations on structural and magnetic properties of cobalt ferrite/ silica nanocomposites prepared by the coprecipitation method, *J.Magn. Magn. Matter.*,2011, **323**,p 897-902
- [7]. Alison E. Deatsch, Benjamin A. Evans, Heating efficiency in magnetic nanoparticle hyperthermia, *J.Magn. Magn.Matter.*, 2014,**345** ,p163-172
- [8]. C. Murugesan, M. Perumal, G. Chandrasekaran, Structural, dielectric and magnetic properties of cobalt ferrite prepared using auto combustion and ceramic route, *Physica B: Condens. Matter*2014 , **448**, p 53-56

- [9]. Y. Cedeno-Mattei, O. Perales-Prerez, Synthesis of high-coercivity cobalt ferrite nanocrystals, *Microelectron. J.*,2009,**40**, p 673-676
- [10]. Bronislav E. Kashevsky, Vladimir E. Agabekov, Sergei B. Kashevsky, Katsiaryna A. Kekalo, Elena Yu. Manina, Igor V. Prokhorov, Vladimir S. Ulashchik, Study of cobalt ferrite nanosuspensions for low-frequency ferromagnetic hyperthermia, *Particuology*2008 **6**,p 322-333
- [11]. P. C. Fannin, C. N. Marin, I. Malaescu, N. Stefu, P. Vlazan, S. Novaconi, P. Sfirloaga, S. Popescu, C. Couper, Microwave absorbent properties of nanosized cobalt ferrite powders prepared by coprecipitation and subjected to different thermal treatments. *Mater.Des.*,2011, **32**, p1600-1604
- [12]. SC. Nian, SW. Tsai, MS. Huang, RC. Huang, and CH. Chen, Key parameters and optimal design of a single-layered induction coil for external rapid mold surface heating, *Int. J. Heat Mass Transfer*,2014,**57**, p109-117
- [13]. T. Ahara, H. Aono, K. Shirai, T. Maehara, H. Hirazawa, S. Matsutomo, Y. Watanabe, High-frequency induction heating of Ti-coated mild steel rod for minimally invasive ablation therapy of human cancer, *J. Magn. Magn. Matter*2013,**331**, p168-173
- [14]. M. Col, M. Yilmaz, The determination of heat treatment parameters of X52 microalloyed steel after high frequency induction welding. *Mater.Des.*,n 2006 **27**, p 507-512
- [15]. G. H. Royer, A switching transistor DC to AC converter having an output frequency proportional to the DC input voltage, *AIEE Trans. Comm. and Elect.*,1955, **74**, p 322-326
- [16]. G. Kirubakaran, R. Kumar, M. Padmanaban, S. Parameswari, Implementation of Royer oscillator in WI-Tricky for low power transfer. *Proceedings of IRF International Conference, Goa, 2014*
- [17]. J.D. van Wyk, J.A. Ferreira, On overcoming the disadvantages of the self-oscillating Royer inverter, *IEE International Conference on Power Electronics and Variable Speed Drives*,1984 London, p 123-126
- [18]. J.A.Ferreira, Van der Broeck, H.W., Bendien, J.C, A self-oscillating bidirectional DC to DC converter employing minimum circuitry, *Power Electronics and Variable-Speed Drives, Third International Conference on IET, July*, p 125-129,1998.
- [19]. Wang et al. United States Patent Application Publication, Pub. No. US 2014/0177291 A1, 2014.
- [20]. R. Ghosh, L. Pradhan, Y. P. Devi, S. S. Meena, R. Tewari, A. Kumar, S. Sharma, N. S. Gajbhiye, R. K. Vatsa, B.N. Pandey and R. S. Ningthoujam, Induction heating studies of Fe₃O₄ magnetic nanoparticles capped with oleic acid and polyethylene glycol for hyperthermia, *J. Mater. Chem.*,2011, **21**, p 13388-13398
- [21]. R. E. Rosensweig, Heating magnetic fluid with alternating magnetic field, *J.Magn. Magn.Matter.*, 2002,**252**, p 370-374
- [22]. R. Hergt, R. Hiergeist, I. Hilger, W. A. Kaiser, Y. Lapatnikov, S. Margel, U. Richter. Maghemite nanoparticles with very high AC-losses for application in RF-magnetic hyperthermia, *J. Magn. Magn.Matter* 2004., **270**p 345-357.
- [23]. Sunghyun Yoon, Temperature dependence of magnetic anisotropy constant in cobalt ferrite nanoparticles, *J. Magn. Magn.Matter.*, 2014**324**, p 2620-2624
- [24]. Rudolf Hergt, Silvio Dutz, Magnetic particle hyperthermia- biophysical limitations of a visionary tumor therapy, *J. Magn. Magn.Matter.*, 2007, 311, p 187-192
- [25]. Branka Babic-Stojic, Vukomon Jokanovic, Dusan Milivojevic, Zvonko Jaglicic, Darko Makovec, Natasa Jovic, and Milena Marinovic-Cincovic, Magnetic and structural studies of CoFe₂O₄ nanoparticles suspended in an organic liquid, *J. Nanomaterials*, 2013,doi:10.1155/2013/741036
- [26]. Jonathan David Paolucci, Novel Current-Fed Boundary-Mode Parallel-Resonant Push-Pull Converter, Faculty of California Polytechnic State University, San Luis Obispo, June 2009
- [27]. Scott Logan McClusky, High voltage resonant self-tracking current-fed converter, Faculty of California Polytechnic State University, San Luis Obispo March 2010.
- [28]. Hosotani T. US Patent #6061252, filed Dec. 1998.
- [29]. Hosotani T, Harada K, Ishihara Y, Todaka T, Self-oscillating voltage-clamped zero-voltage-switching flyback converter, *Trans IEICE; J86-B:837-845*, 2003
- [30]. Tatsuya Hosotani, Kazurou Harada, Yoshiyuki Ishihara, and Toshiyuki Todaka Self-Excited Continuous Conduction Mode ZVS Flyback Converter, *Electronics and Communications in Japan, Part 1*,2004, **88**, p 1798-1806
- [31]. Jaycar Electronics Reference Data Sheet: Understanding & using DC-AC inverters. *Inverter. PDF (1) 2000*
- [32]. T. L. Floyd, *Electronics Fundamentals: Circuits, devices, and applications*, Seventh Edition. Pearson Prentice Hall 2007 p.483.
- [33]. Vishay "General technical information". 26033 -201334. Dong-Hyun Kim, David E. Nikles, Duane T. Johnson, Christopher S. Brazel, Heat generation of aqueously dispersed CoFe₂O₄ nanoparticles as heating agents for magnetically activated drug delivery and hyperthermia, *J. Magn. Magn. Matter* **320**, 2390- 2396, 2008
- [34]. E. Garaio, J. Collantes, J. Garcia, F. Plazaola, S. Mornet, F. Couillaud, O. Sandre, A wide-frequency range AC magnetometer to measure the specific absorption rate in nanoparticles for magnetic hyperthermia, *J.Magn. Magn.Matter.*,2014,**368**, 432-437
- [35]. R. Hiergeist, W. Andra, N. Buske, R. Hergt, I. Hilger, U. Richter, W. Kaiser, Application of magnetic ferrofluids for hyperthermia, *J.Magn. Magn. Matter.*,1999, **201**p 420-422
- [36]. Young, Hugh D., *University Physics*, 7th Ed., Addison Wesley, 1992 chap 15
- [37]. B-D-Cullity, "Elements of X-Ray Diffraction", Addison-Wesley Publishing Company, Inc 1956.149-173
- [38]. Calero-ddelc, Victoria L. A., Carlos Rinaldi, Synthesis and magnetic characterization of cobalt-substituted ferrite (Co_xFe_{3-x}O₄) nanoparticles, *J.Magn. Magn.Matter.*,2007, **314**, p 60-67
- [39]. C. N. Chinnasamy, M. Senoue, B. Jeyadevan, Oscar Perales-Perez, K. Shinoda and K. Tohji, Synthesis of size-controlled cobalt ferrite particles with high coercivity and squareness ratio, *J. Colloid Interface Sci.*,2003, **263**, p 80-83.